Metabolite and Isotopomer Balancing in the Analysis of Metabolic Cycles: II. Applications

Sung M. Park,[1] Maria I. Klapa,[1] Anthony J. Sinskey,[2] Gregory Stephanopoulos[1]

[1]Department of Chemical Engineering, Massachusetts Institute of Technology
[2]Department of Biology, Massachusetts Institute of Technology, Cambridge, Massachusetts 02139

Received 19 December 1997; accepted 24 July 1998

Abstract: In a previous paper (Klapa et al., 1999), we presented a model for the analysis of isotopomer distributions of the TCA cycle intermediates resulting from ^{13}C (or ^{14}C) labeling experiments. Results allow the rigorous determination of the degree of enrichment at specific carbon atoms of metabolites, of the molecular weight distribution of metabolite isotopomers, as well as of the fine structure of NMR spectra in terms of a small number of metabolic fluxes. In this paper we validate the model by comparing model predictions with experimental data and then apply it to the analysis of metabolic networks that have been investigated in previous studies. The results have allowed us to conclude that: (1) there is no evidence of propionyl-CoA carboxylase pathway in *Escherichia coli;* and (2) the possibility that acetone utilization in mammals occurs solely via the ''lactate/methylglyoxal'' pathway is consistent with available labeling data. The presented modeling framework provides additional constraints that must be satisfied by experimental data in a biochemical network structure and therefore enhances the power of labeling methods for resolving in vivo metabolic fluxes. © 1999 John Wiley & Sons, Inc. *Biotechnol Bioeng* **62**: 392–401, 1999.

Keywords: isotopomer analysis; metabolic flux analysis; TCA cycle; ^{13}C NMR; GC–MS

INTRODUCTION

In a previous paper (Klapa et al., 1999), we presented a rigorous mathematical model for the determination of the relative populations of metabolite isotopomers resulting from pyruvate utilization via the tricarboxylic acid (TCA) cycle and the gluconeogenic pathway. In addition, isotopomer distributions for three different models of acetate catabolism were presented. It was further shown how the results of this modeling approach can be used to upgrade the information obtainable from typical NMR spectroscopy measurements. Specifically, it was noted that carbon enrichment data, along with isotopomer molecular weight distributions and the fine structure of NMR spectra at specific carbon positions, can be used to determine in vivo metabolic fluxes and the role they play in meeting biosynthetic and energetic requirements.

In this paper we validate our modeling results by comparing model predictions with experimental data. The model is subsequently applied to the analysis of data from several specific cases reported in the literature. Special emphasis is given to errors associated with the incorrect accounting for possible label scrambling via the TCA cycle. In a future publication the same approach is applied to the analysis of the pentose phosphate pathway, although a numerical approach was followed in the latter case since no analytical expressions for isotopomer distributions could be obtained.

MODEL VERIFICATION

Pyruvate Utilization in Mammals

The validity of our modeling concept can be tested by comparing the model predictions with experimental data. Chance et al. (1983) perfused rat heart tissue with 90% enriched [3-^{13}C]pyruvate and obtained a ^{13}C NMR spectrum which shows resonances and line splittings at the C-2, C-3, and C-4 carbons of glutamate (Fig. 1). The glutamate C-2 resonance is split into nine lines (centered at 55.5 ppm), C-4 is split into three lines (centered at 34.2 ppm), and C-3 is split into five lines (centered at 27.8 ppm). The line splittings are caused by ^{13}C–^{13}C spin coupling among carbon atoms.

With 90% enriched [3-^{13}C]pyruvate as substrate, pyruvate and acetyl-CoA may be either labeled at C-3 and C-2, respectively, or unlabeled. Oxaloacetate produced from labeled pyruvate via the anaplerotic reaction will be labeled at carbon 3, if the bicarbonate is unlabeled, or at carbons 3 and 4, if the bicarbonate is labeled. However, in the oxaloacetate pool will be present also unlabeled oxaloacetate (O) formed from unlabeled pyruvate if the bicarbonate is unlabeled, and isotopomer O_4 if the bicarbonate is labeled. The seven isotopomers of oxaloacetate, O, O_3, O_{34} and O_4, O_2, O_{12} and O_1 (the last three formed because of the equilibrium be-

Correspondence to: G. Stephanopoulos

Contract grant sponsors: National Science Foundation; Department of Energy BES

Contract grant numbers: NSF BCS-9311509; DOE BES DE-FG02-94ER14487

CCC 0006-3592/99/040392-10

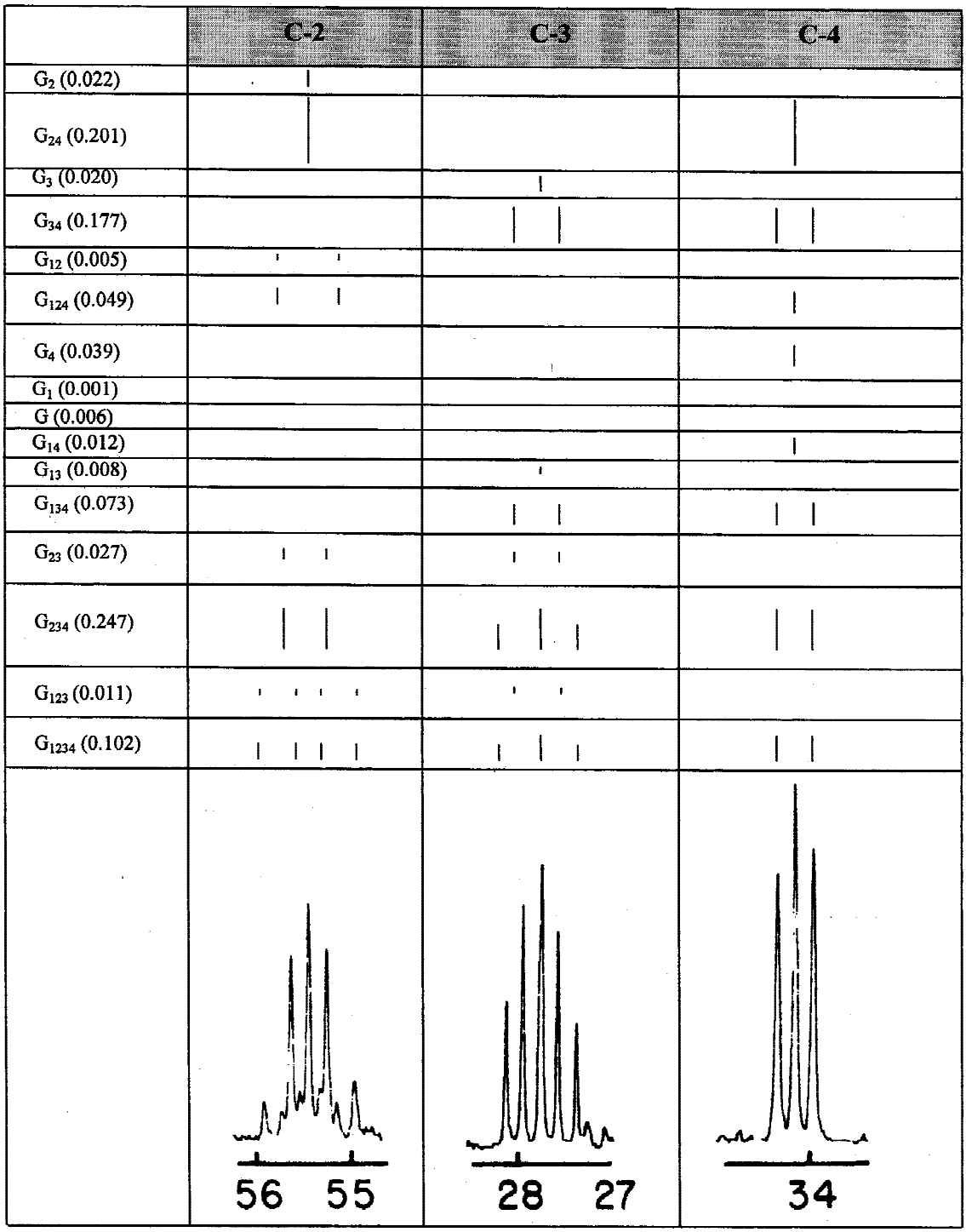

Figure 1. Observed multiplet pattern of glutamate with 90% [3-^{13}C]pyruvate (Chance et al., 1983). The value of *x* is estimated to be equal to 0.35 (see text). The numbers in parentheses are the relative populations of the corresponding isotopomers for this value of *x*. The multiplet due to every isotopomer at carbons 2, 3, and 4 of glutamate is also shown. The intensity of each line within the multiplet should be equal to the relative population of the isotopomer normalized by the number of lines of the multiplet. Superposition of all the multiplets at each carbon atom generates the observed fine structure of the NMR spectra.

tween carbons (2,3) and (1,4)), can condense with labeled (at carbon 2) and unlabeled AcCoA to produce citrate in the TCA cycle. At steady-state, there are 12 isotopomers of oxaloacetate in the oxaloacetate pool: O_4, O_2, O_3, O_{34}, O_{12}, O_{23}, O_{13}, O_{24}, O_{123}, and O_{234}. Accordingly, there are 16 isotopomers in the glutamate pool: G, G_4, G_{14}, G_1, G_{124}, G_{12}, G_{34}, G_3, G_{24}, G_2, G_{234}, G_{23}, G_{134}, G_{13}, G_{1234}, G_{123}.

The occurrence of multiple patterns in the NMR spectrum, presented in Fig. 1, is consistent with the prediction of different isotopomer species. The nine-lines splitting at C-2

is the sum of a singlet (superposition of two different singlets) due to G_{24} and G_2, a doublet with coupling constant J_{12} due to G_{124} and G_{12}, a doublet with coupling constant J_{23} due to G_{234} and G_{23}, and a quartet due to G_{1234} and G_{123}. Two different doublets occur as a result of the difference between the coupling constants J_{12} (53.5 Hz) and J_{23} (34.6 Hz). Because of this difference, the line splitting at C-2 due to G_{1234} and G_{123} is a quartet, whereas the line splitting at C-3 due to G_{1234} and G_{234} is a triplet with an intensity ratio 1:2:1 due to the similar values of J_{23} and J_{34}. For the same reason ($J_{23} = J_{34}$), the isotopomers G_{123}, G_{23}, G_{134}, and G_{34} provide the same doublet at C-3. Thus, the five-lines splitting at C-3 is the sum of a singlet due to G_3 and G_{13}, a doublet due to G_{123}, G_{23}, G_{134} and G_{34}, and a triplet due to G_{1234} and G_{234}. Similarly, the line splitting should be three lines at C-4, three-lines at C-1, and none at C-5. Thus, the fine structure of NMR spectra at all glutamate resonances is consistent with the prediction of the different glutamate isotopomer species.

The intensity of each line is proportional to the sum of the isotopomer concentrations contributing to the corresponding line-splitting (doublet, triplet or quartet), normalized by the number of lines. For example, the intensity of one of the two lines at the doublet at C-2 due to G_{124} and G_{12} is proportional to $([G_{124}] + [G_{12}])/2$, where $[G_i]$ is the concentration of the isotopomer G_i. Using our model [Klapa et al., 1998], the relative distribution of glutamate isotopomer species that determine the line intensity of the NMR spectra, can be calculated uniquely from the values of x (the fraction of OAA entering the TCA cycle) and y (the fraction of bicarbonate fixed in pyruvate, which is labeled with ^{13}C). Assuming that there are no reactions that generate CO_2 other than those depicted in Fig. 1 of (Klapa et al., 1998), the value of y can be determined uniquely from x (see Fig. 2). Predictions of the relative populations of the sixteen glutamate isotopomers for different values of x are shown in Fig. 2.

Since the line intensities of the NMR spectra of Fig. 1 can be determined uniquely from the relative populations of glutamate isotopomers which, in turn, are functions of the flux ratio x, flux information can be extracted from the fine structure of NMR spectra. Any of the three resonances at the C-2, C-3, or C-4 carbons of glutamate can be used for the determination of x, while the other two can be used to validate the estimate of x thus obtained. Table I shows the line intensities ratios as estimated from the NMR spectra of Fig. 1. The relative areas of the multiplets were measured manually from the published NMR spectra by triangulation: peak height × width at half height. The values of x obtained when only one carbon resonance at a time is used is approximately the same as the least-square estimate obtained when all three resonances are used in the calculation, and equal to 0.35 ± 0.01. The corresponding value of y is 0.26 ± 0.01. Table I shows the line intensities ratios calculated for these values of x and y. The satisfactory agreement with the experimental data at all three carbon atoms supports the validity of our modeling methodology. Differences observed between the experimental data and the theoretical predictions at C-2 can be explained by the uncertainty in the estimation of the line intensity ratios from the published NMR spectra of Fig. 1. It is noted that the line intensity

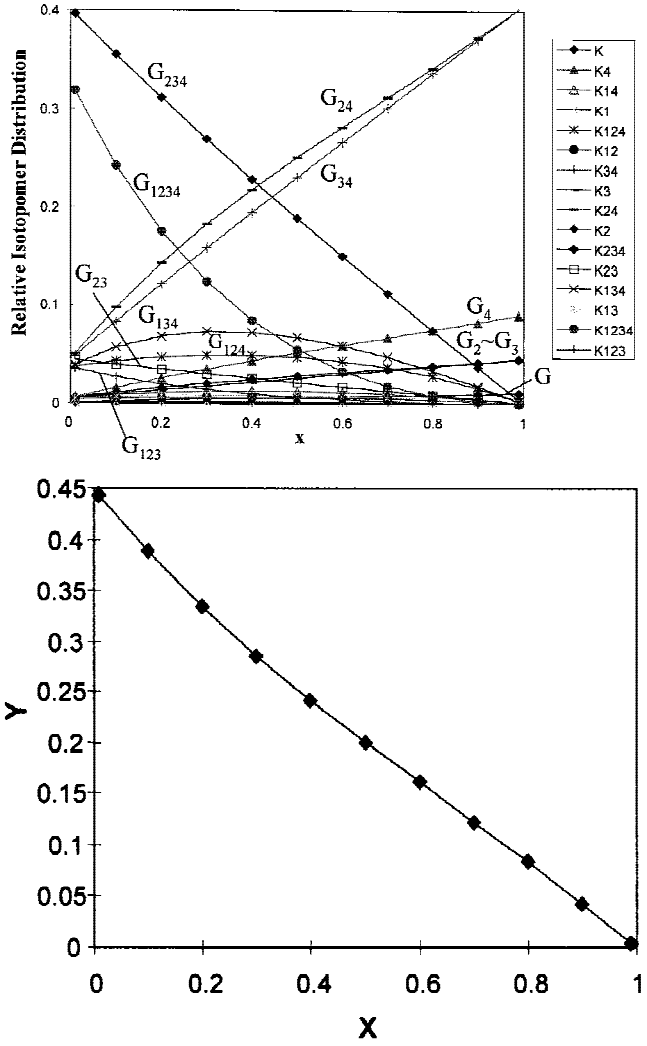

Figure 2. Distribution of α-ketoglutarate isotopomers as a function of x for the case of 90% [3-^{13}C]pyruvate. Sixteen species are present, and y is obtained exclusively as a function of x by assuming that there are no other reactions generating CO_2 than those depicted in Fig. 1 of Klapa et al. (1998).

Table I. Determination of flux ratio x from the line intensities of the NMR spectra of Figure 1.

	C-2			C-3	C-4
	S/D12	S/D23	S/Q	T/D	S/D
NMR spectrum	4.20 ± 0.3	0.73 ± 0.1	1.95 ± 0.3	1.3 ± 0.1	0.5 ± 0.2
x = 0.35	*4.13*	*0.81*	*1.97*	*1.3*	*0.5*

Note. The best estimate for x is 0.35. The values in italics represent the line intensities ratios calculated for this value of x. (S, D, and T are the intensities of the singlet, of the doublet (both lines) and of the triplet (all three lines), respectively; D_{ij} is the intensity of the doublet with coupling constant J_{ij}).

ratios at the other two carbon atoms calculated for $x = 0.35$ fall within the range of experimental error. Similar multiplet patterns in glutamate and glutamine were also obtained in isolated livers of mice perfused with [3-^{13}C]alanine by Hall et al. (1988).

Acetate Utilization in *E. coli*

Our modeling results can be verified in another system. Walsh and Koshland (1984) obtained a ^{13}C NMR spectrum of purified glutamate from *E. coli* grown with 99% [2-^{13}C]acetate as the sole carbon source (Fig. 3). It shows a doublet at C-1, a six-lines at C-2, a triplet at C-3, and a doublet at C-4. This pattern is consistent with the operation of the glyoxylate shunt pathway (Model I) and exactly matches the predictions of Table 2 of Klapa et al. (1998). There is only one variable in this case, *z*, that essentially determines the relative intensity of each peak and each line within each peak. *z* is defined as the probability of isocitrate utilized via the glyoxylate shunt pathway (or the fraction of isocitrate utilized in the glyoxylate pathway, the balance being converted in the TCA cycle). According to Walsh and Koshland, the relative enrichment at the five carbons of intracellular glutamate was 0.4:1.0:0.9:1.0:0 for C-1 through C-5, respectively. Our model predicts C-2 = C-3 = C-4 = 1 and C-5 = 0, which are in total agreement with the experimental results, whereas C-1 = $(1 - z)/2$. Inserting the experimental value of 0.4 for C-1, *z* is calculated equal to 0.2. This is identical to the value estimated by Walsh and Koshland using an involved method based on input–output equations for each carbon on intermediary metabolites.

Our model results can also explain exactly the fine structure of the obtained NMR spectra, since we consider all the isotopomers of the intermediate metabolites and not just isotope enrichment at specific metabolite carbon positions. Even though the labeling diagram (Fig. 6 of Klapa et al. [1999]), shows the presence of up to six α-ketoglutarate isotopomers, the results of Table II of Klapa et al. (1998) show that, under steady state, only two α-ketoglutarate species should be present: K_{1234} (or G_{1234}) with a relative population of $(1 - z)/2$ and K_{234} (or G_{234}) with a relative population $(1 + z)/2$. The multiple pattern can be analyzed in a manner similar to the case of [3-^{13}C]pyruvate of section 2.1. Of particular interest is the pattern at C-2. Here G_{1234} should give rise to a quartet at C-2 with each line intensity $(1 - z)/8 = 0.1$, and G_{234} should give a doublet at C-2 with each line intensity $(1 + z)/4 = 0.3$. These predictions cannot be compared directly with the results of Fig. 3 due to lack of intensity data for the individual peaks of the C-2 resonance. However, comparison of the heights of the individual peaks shows general agreement between experimental and predicted values. The intensities at the C-3 and C-4 resonances can be similarly analyzed. They contain no information for the value of the flux ratio *z*, however, they are very consistent with the above patterns. Similar labeling patterns were observed in glutamate by *Brevibacterium flavum* (Walker and London, 1987) and proline, which also reflects exact labeling pattern of α-ketoglutarate by *E. coli* (Crawford et al., 1987).

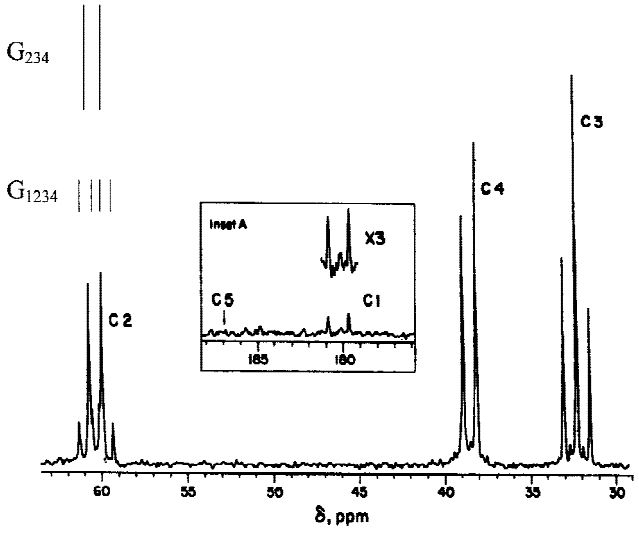

Figure 3. Observed glutamate multiplet patterns with [2-^{13}C]acetate (adopted from Walsh and Koshland [1984]). Peak at C2 is a six-lines consisting of a doublet due to G_{234} with each line intensity 0.3 and a quartet due to G_{1234} with each line intensity 0.1 for a value of *z* equal to 0.2.

Another experiment for verifying the operation of the glyoxylate shunt pathway in bacteria was performed with 99% [1-^{13}C]acetate. In this case too the glutamate isotopomer species can be obtained in terms of *z*. Only two species should be present (Table III of Klapa et al. [1998]): G_5 with relative population $(1 + z)/2$ and G_{15} with relative population $(1 - z)/2$. Therefore, enrichment of glutamate should be $(1 - z)/2$ at C-1, 1 at C-5, and 0 at C-2, C-3, and C-4. This is exactly what is observed in proline synthesis by *E. coli* (Crawford et al., 1987) and glutamate synthesis by *B. flavum* (Walker and London, 1987). Since the system of (Crawford et al., 1987) was similar to that of (Walsh and Koshland, 1984), one can assume the same value for $z = 0.2$ that yields an estimate for glutamate C-1 enrichment of 0.4. From the spectra reported in (Crawford et al., 1987), the C-1 glutamate enrichment can be estimated as 30%, in fair agreement with the model estimates.

APPLICATIONS

Pathway of Acetate Utilization in *Pseudomonas* AM1

Narbad et al. (1989) concluded the absence of the glyoxylate shunt pathway in the methylotrophic *Pseudomonas* AM1 strains by examining the distribution of ^{13}C label in trehalose formed from [2-^{13}C]acetate. Their conclusion was based on the labeling pattern of trehalose, which reflects glucose patterns: C-1:C-2:C-3:C-4:C-5:C-6 = 35.8:33.86:24.15:24.43:37.58:37.0. They argued that since trehalose derived from oxaloacetate via glyoxylate cycle activity only would not be labeled at C-3 and C-4 and operation of the TCA cycle would label the C-3 and C-4 positions of treha-

lose at 50% intensity of the other sites, the intensities of C-3 and C-4 of trehalose of 70% of the levels of the other four carbon atoms rule out the operation of the glyoxylate shunt. This conclusion is consistent with experimental observations indicating lack of isocitrate lyase activity (Dunstan et al., 1972a,b).

Our model is consistent with the above conclusion. Considering the network of Fig. 7 in Klapa et al. (1999), but with 90% enriched acetate, the possible oxaloacetate isotopomers are O, O_2, O_3, O_{23}, O_1, O_4, O_{13}, O_{24}, O_{12}, O_{34}, O_{123}, and O_{234}. The relative intensity of O-1:O-2:O-3 and consequently of C-3:C-2:C-1 of glucose was calculated to be $(1 - z)/2:1:1$, which is consistent with what is concluded by Narbad et al. The maximum value of the C-3/C-2 ratio is 50%, when $z = 0$ or the glyoxylate shunt is inactive. The relative intensity of O-1:O-2:O-3 for 90% enriched acetate turns out to be the same with respect to the ratio z for 100% enriched acetate (see Table II, Model I of Klapa et al. (1999)).

On the other hand, introducing the relative intensity of C-1:C-2:C-3 of glucose, as determined experimentally: 1:1:0.7, in the expressions of Model II (Table II of Klapa et al. (1999)) (we consider that the formation of extra isotopomers, because of 90% enriched acetate, is not affecting considerably the relative intensity of the glucose carbons), we calculate the ratio x equal to 0.8. Thus, if we consider the pyruvate carboxylation reaction as the alternative anaplerotic pathway, the experimentally measured label pattern of glucose is consistent with low activity of the TCA cycle.

Pathway of Acetate Utilization in Mammals

Many researchers have described acetate metabolism in mammals using labeled acetate under various conditions (Table II). Predominately monitored substrates are glutamate and/or glucose. Qualitatively, with C-1 labeled acetate, the possibility of the operation of Model III can be distinguished from that of either Model I or Model II by following the carbon enrichments of glutamate or glucose (Table III of Klapa et al. (1999)). With Model III, all six carbons of glucose are expected to be labeled whereas with Model I or Model II, only C-3 of glucose is labeled. Similarly with Model III four carbons of glutamate, namely C-1, C-2, C-3, and C-5, are labeled, whereas with Model I or Model II label is present in only at C-1 and C-5. The data of Table II excludes the possibility of Model III in mammals. It must be noted that with C-1 labeled C_2 metabolites, Model I and Model II cannot be differentiated.

The same analysis can be applied with C-2 labeled acetate based on Table 2 of Klapa et al. (1999). Qualitatively, all three models lead to same labeling patterns in the carbons of glutamate and glucose. Quantitatively, Model I can be differentiated from Model II. For example, the relative enrichments at C-2, C-3, and C-4 of glutamate are all equal to 1 with Model I. With Model II, only the enrichment at C-4 of glutamate is equal to 1. According to Model II, C-2 and C-3 of glutamate and C-1 and C-2 of glucose should be labeled with intensity $(1 - x)/(1 + x)$. The data in Table II support the operation of Model II.

With C-2 labeled acetate, the distinction between Model II and Model III cannot be unequivocally established from either the qualitative or quantitative analysis of the relative enrichment data. However, the multiple pattern structure in the ^{13}C NMR spectrum should be different. If acetate is utilized solely via the acetyl-CoA conversion pathway (Model II), the resulting multiple pattern at glutamate should appear as: three-lines at C-1 consisting of a singlet due to G_{14} and G_{134}, a doublet due to G_{1234}; seven-lines at C-2 consisting of a singlet due to G_{24}, a doublet due to G_{234}, and a quartet due to G_{1234}; five-lines at C-3 consisting of a doublet due to G_{34} and G_{134} and a triplet due to G_{234} and G_{1234}; and three-lines at C-4 consisting of a singlet due to G_4, G_{14}, and G_{24} and a doublet due to G_{34}, G_{134}, G_{234}, and

Table II. Distribution of ^{14}C in the carbons of glutamate or glucose with ^{14}C labeled C-2 metabolites.

	Carbon position						
Substrate	C-1	C-2	C-3	C-4	C-5	C-6	References
[1-^{14}C]Acetate[a]	3	7	48	100	1	1	Antony and Landau, 1968
[1-^{14}C]Acetate[b]	1	2	65	100	2	1	Kam et al., 1978
[1-^{14}C]Ethanol[c]	28.0		0.0		71.8		Schumann et al., 1991
[2-^{14}C]Acetate[d]	57	57	16	23	94	100	Antony and Landau, 1968
[2-^{14}C]Acetate[e]	12.1	21.3	22.7	42.9	1.0		Schumann et al., 1991
[2-^{14}C]Acetate[f]	18.5	18.8	11.4	11.9	19.3	20.4	Schumann et al., 1991
[2-^{14}C]Acetate[g]	11.0	23.6	24.4	37.8	1.9		Hill et al., 1958
[2-^{14}C]Acetate[h]	73.7	68.3	15.3	16	100	92.3	Kam et al., 1978

[a] ^{14}C specific activity in glucose normalized by specific activity in C-4 of glucose from rat liver.
[b] ^{14}C specific activity in glycogen normalized by specific activity in C-4 of glucose from 72-h fasted monkey liver slices.
[c] % in carbons of glutamate from urinary phenylacetylglutamine. One sample at time 3–6 h.
[d] ^{14}C specific activity in glucose normalized by specific activity in C-6 of glucose from rat liver.
[e] % in carbons of glutamate from urinary phenylacetylglutamine. Average of four samples at time 4.5–6 h.
[f] % in carbons of glucose in blood. Average of four samples at time 6 h.
[g] % in carbons of glutamate from rat carcuss.
[h] ^{14}C specific activity in glycogen normalized by specific activity in C-4 of glucose from 72-h fasted monkey liver slices. Average of three samples.

G_{1234}. A nearly identical multiple structure is expected in Model III. The major difference is at C-2 which should be a nine-lines peak with an additional doublet due to G_{124}. These candidate pathways can be differentiated using our model due to its enumeration of the possible metabolite isotopomers.

Pathway of Propionate Utilization in *E. coli*

Evans et al. (1993) attempted to establish the operation of dual pathways for propionate utilization in *E. coli* using ^{13}C NMR with [2-^{13}C]propionate and [3-^{13}C]propionate as the sole carbon substrate. In *E. coli,* propionate is oxidized to pyruvate which then enters the TCA cycle either as acetyl-CoA via the action of pyruvate dehydrogenase or as OAA via the sequential actions of PEP synthetase and PEP carboxylase. However, in several systems including higher organisms and a number of microorganisms such as *Propionibacterium* (Wood and Stjernholm, 1961), *Ochromonas* (Arstein et al., 1962), and *Rhizobium* (De Hertogh et al., 1964), the major pathway of propionate metabolism is via the propionyl-CoA carboxylation pathway. In such systems, propionate is converted to propionyl-CoA, which is then carboxylated to methylmalonyl-CoA via propionyl-CoA carboxylase, which is finally isomerized to succinyl-CoA via methylmalonyl-CoA mutase. With [2-^{13}C]propionate, Evans et al. obtained a ^{13}C NMR spectrum (Fig. 4) which shows a singlet at all five carbons of glutamate with relatively high enrichment at C-1 and C-5 positions, and low enrichment at C-4 position. They argued that if [2-^{13}C]propionate is solely utilized via the pyruvate pathway, no C-2 and C-3 of glutamate should be labeled. However, since C-2 and C-3 were also significantly labeled, it was concluded that a propionate carboxylation pathway must be operative in this bacterium, which they supported to be the propionyl-CoA carboxylase pathway. Clearly this is incorrect as the argument is made on the model that describes the label distribution, when pyruvate enters the TCA cycle only through acetyl-CoA and the pyruvate carboxylase activity is ignored. Considering the action of both pyruvate dehydrogenase and pyruvate carboxylase, the labeling pattern of glutamate is consistent with the sole operation of the pyruvate pathway (Table I, Column 2 of Klapa et al. (1999)). Furthermore, in another experiment with [3-^{13}C]propionate (Fig. 4), a labeling pattern consistent with a multiple pattern associated with the sole operation of the pyruvate pathway (Table I, Column 1 of Klapa et al. (1999)) was found. Therefore, the operation of the propionyl-CoA carboxylase pathway in *E. coli* cannot be substantiated with the ^{13}C NMR study.

Pathway of Acetone Utilization in Mammals

The metabolic pathways of acetone utilization in mammals remains unclear despite its presumed importance in diabetic ketoacidosis where large amounts of acetone, along with acetoacetate and 3-hydroxybutyrate, accumulate in the body fluids (Sulway and Malins, 1970; Owen et al., 1982). Another important question associated with acetone metabolism is how much energy can be derived from acetone during fasting in order to prolong survival. Reichard et al. (1979) calculated that up to 11% of the glucose can be

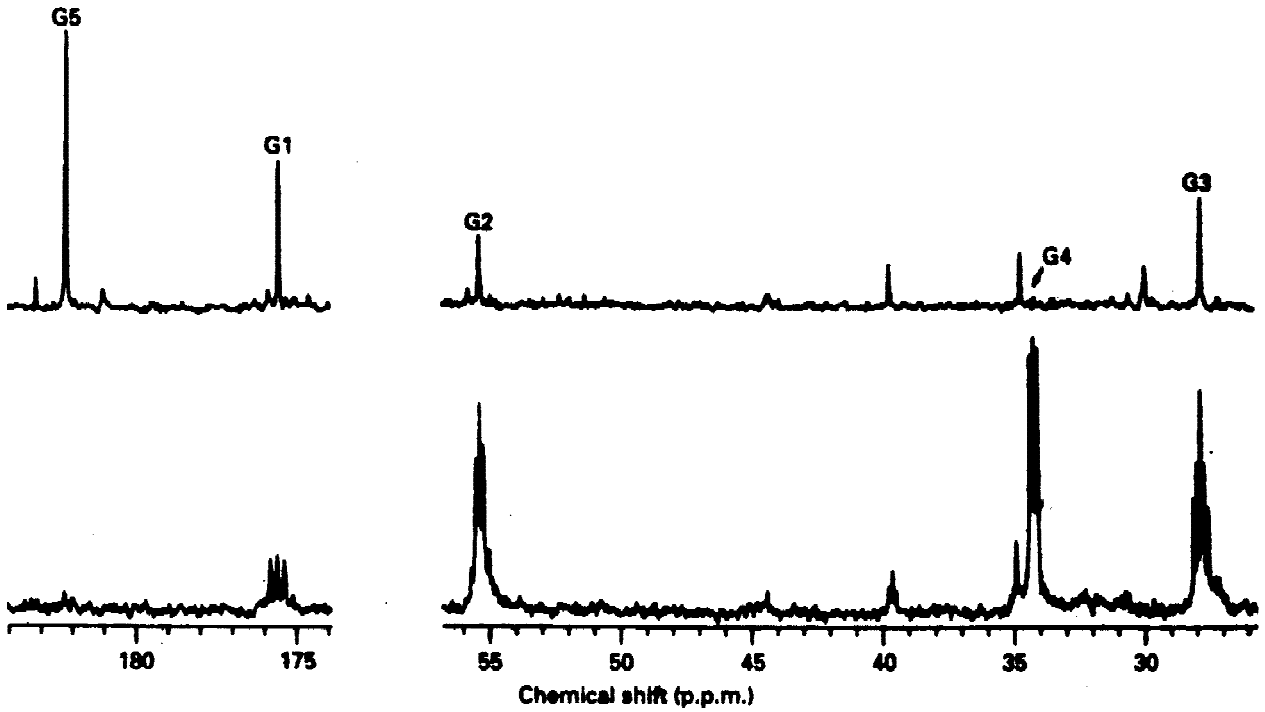

Figure 4. Glutamate multiplet pattern observed in *E. coli* with [2-^{13}C]propionate (top) and [2-^{13}C]propionate (bottom) (adopted from Evans et al. [1993]).

derived from acetone during starvation in humans. Previously acetone was considered a non-metabolizable end product of lipid metabolism that accumulates when there are insufficient glycolytic intermediates to effect the complete oxidation of the acetyl-CoA generated in the metabolism of fatty acid. Sakami and Lafaye (1951) proposed two pathways for acetone metabolism in mammalian systems (Fig. 5). One pathway involves the conversion of acetone to 1,2-propanediol which is then cleaved into acetate (C_2 metabolite) and formate. Acetate is then further oxidized via the pathway in Model II (Fig. 2. of Klapa et al. (1999)). The other pathway allows for acetone conversion into C_3 metabolites, namely pyruvate, hydroxyacetone, propanediol, hydroxypyruvate, lactaldehyde, lactate, or their phosphorylated derivatives as possible intermediates.

To delineate which of the two acetone pathways (Fig. 5) is active in acetone metabolism, many researchers used [^{14}C]acetone and followed label incorporation in glucose and glutamate. Casazza et al. (1984) proposed the conversion of acetone into methylglyoxal and 1,2-propanediol with lactate as an intermediate, since he found that cyanamide (an aldehyde dehydrogenase inhibitor) prevents completely the conversion by hepatocytes of 1,2-propanediol to glucose, but inhibits the conversion of [2-^{14}C]acetone to glucose only by 20–40%. Based on findings that there was no carbon label incorporation from [2-^{14}C]acetone into lactate and 3-hydroxybutyrate but significant label incorporation in C-1 of free acetate, Gavino et al. (1987) claimed that in perfused rat livers, acetone metabolism proceeds mainly via the ''acetate'' pathway. Kosugi et al. (1986), based on a study with [2-^{14}C]acetone in humans, concluded the simultaneous operation of both ''lactate/methylglyoxal'' and ''acetate'' pathways. They also claimed that the extent to which either pathway is utilized is based on the concentration of acetone infused, not the dietary state or the prior exposure to acetone. They found that when trace quantities were administered, only small equal percentages of ^{14}C were found in C-3 and C-4 of glucose and large percentages were distributed equally in C-1, C-2, C-5, and C-6 of glucose. However, upon infusion of large quantities of [2-^{14}C]acetone, the reverse effect was found: large percentages were found in C-3 and C-4 and small percentages were found in C-1, C-2, C-5, and C-6 of glucose. Since the conversion of [2-^{14}C]acetone to [1-^{14}C]acetate will label exclusively C-3 and C-4 of glucose (Table III, Model II of Klapa et al. (1999)), whereas the conversion to [2-^{14}C]lactate will label all six carbons of glucose (Table II of Klapa et al. (1999)), Kosugi's data clearly eliminate the possibility of the sole utilization of acetone via the ''acetate'' pathway. Kosugi et al. concluded that at high concentrations the conversion to acetate predominates whereas at low concentrations the conversion to lactate/methylglyoxal predominates. Their conclusion was based also upon experiments introducing simultaneously lactate and acetone or lactate only to the organisms. Assuming that metabolism reacts similarly in both cases, they eliminate the possibility of the sole utilization of ''lactate/methylglyoxal'' pathway because the results from the two experiments were different.

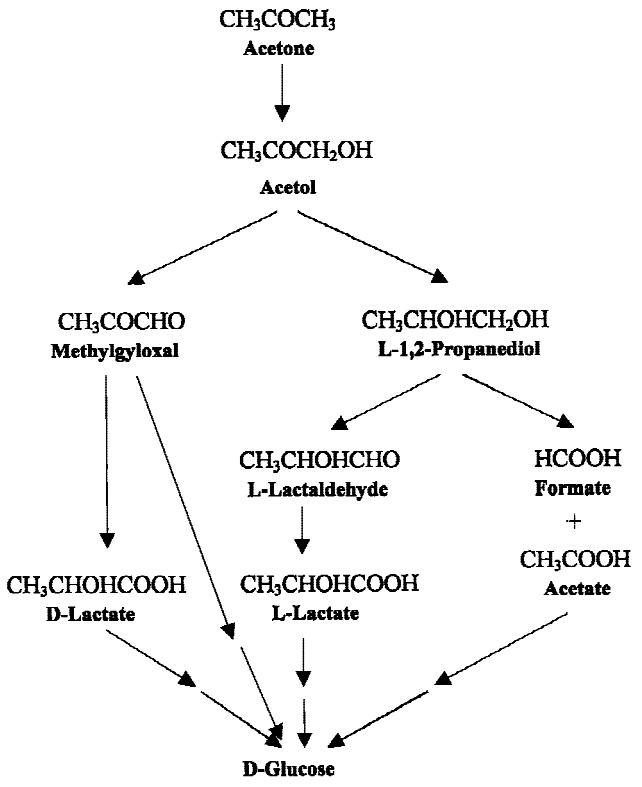

Figure 5. Postulated pathways in the conversion of acetone to glucose (adopted from Kosugi et al. (1986)), (1) involving C_3 metabolites such as methylglyoxal, D-lactate, L-lactate, and L-lactaldehyde and (2) involving C_2 metabolite, acetate.

However, the conditions under which the activation of ''acetate'' pathway is taking place have to be very carefully examined because the larger percentage of label in C-3 and C-4 than in C-1, C-2, C-5, and C-6 of glucose can be interpreted on the basis of the sole operation of ''lactate/methylglyoxal'' pathway. As shown in Fig. 6, at a low value of *x* which corresponds to high TCA cycle activity, the label incorporation at C-1 and C-2 of glucose should be lower than that of C-3 of glucose, whereas the reverse is true at high value of *x.* A high TCA cycle activity may be invoked as a detoxification mechanism at high levels of acetone whereas at low concentrations of acetone, a low TCA cycle is needed.

Reichard et al. (1986) who perfused small amount of [2-^{14}C]acetone into human with diabetic ketoacidosis obtained results similar to those of Kosugi et al. At low acetone infusion, they found that in six of seven patients, 70% to 90% of ^{14}C resides in C-1, C-2, C-5, and C-6 positions. However, in one patient they found more ^{14}C incorporation in C-3 and C-4 than in C-1, C-2, C-5, and C-6 of glucose. This led them to suggest that other pathways of acetone metabolism may exist among subclasses of diabetic patients. However, it is very likely that the source of variation was the rate of the acetone utilization via the TCA cycle, not that an alternate pathway was involved. This particular pa-

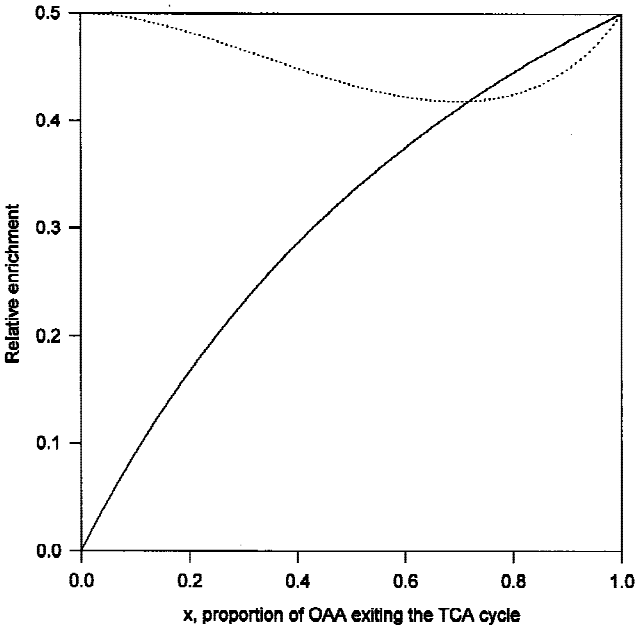

Figure 6. Carbon enrichment in glutamate and glucose as a function of x with [2-^{13}C]pyruvate as substrate. The enrichments at C-1 and C-2 of glucose and C-2 and C-3 of α-ketoglutarate are equal and represented as a solid line. The enrichments at C-3 of glucose and C-1 of α-ketoglutarate are equal and represented as a dotted line.

tient carried a hypertensive cardiovascular disease which is normally associated with high TCA cycle activity.

Thus on the basis of the acetone labeling study in mammals, (1) the possibility of acetone utilization sole via the ''acetate'' pathway can be eliminated, (2) the possibility that acetone utilization occurs solely via the ''lactate/methylglyoxal'' pathway and that the concentration of acetone determines the rate of conversion by effecting different rates of the TCA cycle is consistent with carbon label experimental data, and thus (3) the conditions under which ''acetate'' pathway becomes active should be very carefully examined in every system.

Glyoxylate Shunt Pathway versus TCA Cycle in Bacteria

The value of z, indicating the fraction of isocitrate converted via the glyoxylate shunt pathway, can be determined by three independent methods involving the use of GC-MS and ^{13}C NMR. First, as done by Walsh and Koshland (1984), the relative enrichment at glutamate C-1 can be used. This approach requires additional measurement of known standards in order to establish the calibration required for converting the absolute peak intensity into relative enrichment. Secondly, within the C-2 peak, the ratio of quartet (Q) to doublet (D) can be used to find the value of z: $Q/D = (1 - z)/(1 + z)$. From Fig. 3, this ratio is estimated to be equal to ⅔ giving a value of z equal to 0.2, which is the same result obtained with the first method. Thirdly, GC–MS, measuring the fractions of the same metabolite with different molecular weights differentiated by one atomic mass unit, can be used. In the example of Walsh and Koshland (1984), GC–MS should produce two peaks for glutamate, one corresponding to molecular weight (M + 3), and another corresponding to (M + 4), where M represents the molecular weight of glutamate with all its carbons being ^{12}C. The glutamate species, G_{234}, has a molecular weight of (M + 3) and G_{1234}, has a molecular weight of (M + 4). Therefore the ratio of the (M + 3) to (M + 4) species is $(M + 3)/(M + 4) = (1 + z)/(1 - z)$.

Similarly, in the case of [1-^{13}C]acetate, the value of z can be obtained in two different ways: One from the ^{13}C NMR measurement of relative enrichment at each carbon and the GC–MS measurement of the ratio of (M + 2) to (M + 1).

Determination of Flux of Pyruvate Carboxylase versus Flux of Citrate Synthase

Cohen (1987) proposed the following formula to estimate the ratio of pyruvate carboxylase (PC) activity to pyruvate dehydrogenase (PDH) activity with a C-3 labeled three-carbon substrate:

$$\frac{V_{PC}}{V_{PDH}} = \frac{\text{C-2 of glutamate} + \text{C-3 of glutamate}}{\text{C-4 of glutamate}} \quad (1)$$

With a C-2 labeled three-carbon substrate, the formula was modified by Jans and Willem [1989] as:

$$\frac{V_{PC}}{V_{PDH}} = \frac{\text{C-2 of glutamate} + \text{C-3 of glutamate}}{\text{C-5 of glutamate}} \quad (2)$$

These formulas were adopted by Jans and Willem (1988, 1989) in studies of rabbit and rat renal cells of proximal convoluted tubules, Jans and Leibfritz (1988) in renal epithelial cell lines, Tran-Dinh et al. (1991) in *Saccharomyces cerevisiae* and Brand et al. (1992) in rat neuronal and glial tumor and primary cell lines. However, these formulas are based on the assumption that C-2 and C-3 of glutamate can be derived only from the C-2 and C-3 of OAA, and C-4 and C-5 of glutamate can be derived only from C-2 and C-1 of acetyl-CoA. This assumption is true only if all metabolites undergo the TCA cycle once. As can be seen in many of our labeling diagrams, carbon labels can move from C-4 and C-5 of glutamate to C-1, C-2, and C-3 of glutamate.

It should be clear how these relationships should be modified to account for multiple cycle turns following our methodology. We let x be the proportion of OAA entering the TCA cycle via citrate synthase and $(1 - x)$ as the proportion of OAA exiting the TCA cycle. It should be noted that under the steady state assumption, the flux via citrate synthase is equal to the flux via the pyruvate dehydrogenase, and the flux via the PEP carboxykinase is equal to the flux of pyruvate carboxylase. The above ratio can be represented as

$$\frac{V_{PC}}{V_{PDH}} = \frac{x}{1 - x} \quad (3)$$

The expression for x can be obtained exclusively as a function of enrichment. For the C-3 labeled substrate from Table 1 of Klapa et al. (1999), this is equal to

$$\text{C-2 (or C-3) of glutamate} = \frac{1}{1+x} \tag{4}$$

Hence,

$$\frac{V_{PC}}{V_{PDH}} = \frac{1 - \text{C-2 (or C-3) of glutamate}}{2 \times \text{C-2 (or C-3) of glutamate} - 1} \tag{5}$$

Similarly, for the C-2 labeled substrate, this is related to:

$$\text{C-2 (or C-3) of glutamate} = \frac{x}{1+x} \tag{6}$$

$$\frac{V_{PC}}{V_{PDH}} = \frac{\text{C-2 (or C-3) of glutamate}}{1 - 2 \times (\text{C-2 (or C-3) of glutamate})} \tag{7}$$

Figure 7a and b compare the predictions of the ratio V_{PC}/V_{PDH} as a function of x based on the Cohen's (Eqs. (1) and (2)) and our formulas (Eqs. (5) and (7)) for C-2 and C-3 labeled substrates. It can be seen that the two predictions are exactly opposite for C-3 labeled substrates, but are qualitatively similar for C-2 labeled substrates for values of x up to approximately 0.4.

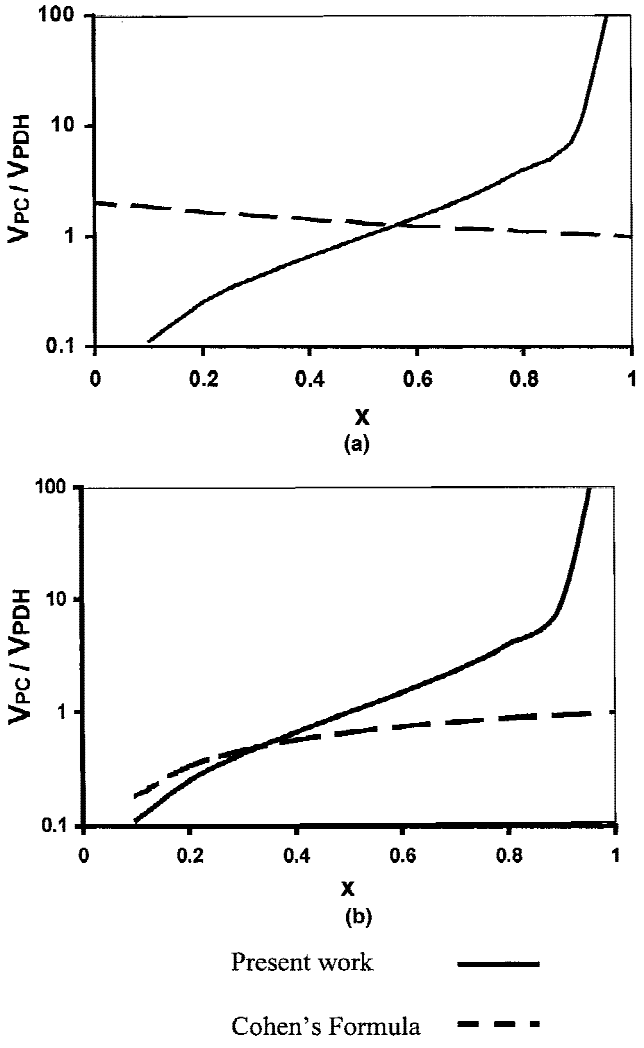

Figure 7. Predictions of the ratio of V_{PC}/V_{PDH} as a function of x according to Cohen's and our formulas for (a) [3-^{13}C]pyruvate and (b) [2-^{13}C]pyruvate as substrate.

The conclusions based on the use of Cohen's formula should be reexamined. For example, Tran-Dinh et al. (1991) observed much smaller enrichment in C-2 of glutamate but the same enrichment in C-4 of glutamate when *S. cerevisiae* is incubated with amphotericin B, a polyene fungal antibiotics, and [1-^{13}C]glucose which leads to the formation of [3-^{13}C]pyruvate. Based on the use of the Cohen's formula, Tran-Dinh et al. concluded that amphotericin B induces a reduction in the pyruvate carboxylase activity in the mitochondria and therefore the effect of amphotericin B should be mitochondrial. However, with our formula, the data can be interpreted as a reduction in either citrate synthase or pyruvate dehydrogenase activity which means that the effect of amphotericin B should be cytosolic. A similar misinterpretation was made by Brand et al. (1992) who observed a higher (C-2 + C-3)/C-4 ratio in primary glial cells than neurons and concluded that there was a higher pyruvate carboxylase activity in primary glial cells than neurons. In fact, the exact opposite could be true.

CONCLUSION

It must be apparent that ^{13}C or ^{14}C labeling data provides unique information about cellular metabolism in a continuous, noninvasive manner. This potential, however, can be realized only if the data is analyzed and interpreted within a proper framework. We have constructed a mathematical model to describe the isotopomer distribution via the TCA cycle and gluconeogenic pathway. Our present modeling approach is similar to earlier models in that each isotopomer species is treated as distinct, independent variable constrained by the topology of enzymatic reactions. In addition, metabolite labeling resulting from multiple TCA cycle turns has been accounted for. Steady state expressions for the distribution of isotopomer species are obtained exclusively in terms of flux variables. Based on isotopomer analysis, we have illustrated several ways to extract the relevant and useful information from the labeling studies. In the case of monitoring with ^{13}C NMR, we have shown how our results can be used in interpreting the complex multiplet patterns of NMR spectra. Alternatively, we have shown a rigorous way of determining flux values from ^{13}C NMR and GC–MS measurements.

Our modeling results are compared to several published experimental data involving different labeled substrates in order to validate our modeling methodology and shown to fit well with the data. These results were extended to investigate the validity of conclusions which were built upon the simplified model that does not properly account for all possible effects of label scrambling via the TCA cycle. Those comparisons led us to confirm that the glyoxylate shunt

pathway does not operate in *Pseudomonas* AM1 strain, and to conclude that (1) there is no evidence of propionyl-CoA carboxylase pathway in *E. coli*, and (2) acetone utilization in mammals solely via the ''lactate/methylglyoxal'' pathway is consistent with published labeling data.

NOMENCLATURE

G	glutamate
Glu	glucose
K	α-ketoglutarate
O, OAA	oxaloacetate
PC	pyruvate carboxylase
PDH	pyruvate dehydrogenase
PEP	phosphoenolpyruvate
TCA	tricarboxylic acid cycle
V_i	flux through enzyme *i*
x	probability of oxaloacetate to exit the TCA cycle
$(1 - x)$	probability of oxaloacetate to enter the TCA cycle
y	probability of bicarbonate to be labeled with ^{13}C
z	probability of isocitrate to be utilized via the GS pathway
$(1 - z)$	probability of isocitrate to be utilized via the TCA cycle

Support by the National Science Foundation (Grant No. BCS-9311509) and the Department of Energy BES (Grant No. DE-FG02-94ER14487) is gratefully acknowledged.

References

Antony GJ, Landau BR. 1968. Relative contribution of α, β-, and ω-oxidative pathways to in vitro fatty acid oxidation in rat liver. J Lipid Res 9:267–270.

Arstein HRV, White AM. 1962. The function of vitamin B_{12} in the metabolism of propionate by the protozoan Ochromonas malhamensis. Biochem J 83:264–270.

Brand A, Engelmann J, Leibfritz D. 1992. A ^{13}C NMR study on fluxes into the TCA cycle of neuronal and glial tumor cell lines and primary cells. Biochimie 74:941–948.

Casazza JP, Felver ME, Veech RL. 1984. The metabolism of acetone in rat. J Biol Chem 259:231–236.

Chance EM, Seeholzer SH, Kobayashi K, Williamson JR. 1983. Mathematical analysis of isotope labeling in the citric acid cycle with applications to ^{13}C NMR studies in perfused rat hearts. J Biol Chem 258:13785–13794.

Cohen SM. 1987. ^{13}C NMR study of effects of fasting and diabetes on the metabolism of pyruvate in the tricarboxylic acid cycle and of the utilization of pyruvate and ethanol in lipogenesis in perfused rat liver. Biochemistry 26:581–589.

Crawford A, Hunter BK, Wood JM. 1987. Nuclear magnetic resonance spectroscopy reveals the metabolic origins of proline excreted by an Escherichia coli derivative during growth of [^{13}C]acetate. Appl Environ Microbiol 53:2445–2451.

De Hertogh AA, Mayeux PA, Evans HJ. 1964. The relationship of cobalt requirement to propionate metabolism in Rhizobium. J Biol Chem 239:2446–2453.

Dunstan PM, Antony C, Drabble WT. 1972. Microbial metabolism of C_1 and C_2 compounds: The involvement of glycollate in the metabolism of ethanol and of acetate by Pseudomonas AM1. Biochem J 128: 99–106.

Dunstan PM, Antony C, Drabble WT. 1972b. Microbial metabolism of C_1 and C_2 compounds: The role of glyoxylate, glycollate and acetate in the growth of Pseudomonas AM1 on ethanol and on C_1 compounds. Biochem J 128:107–115.

Evans CT, Sumegi B, Srere PA, Sherry AD, Malloy CR. 1993. [^{13}C]Propionate oxidation in wild type and citrate synthase mutant Escherichia coli: Evidence for multiple pathways of propionate utilization. Biochem J 291:927–932.

Gavino VC, Sommas J, Philberts L, David F, Garneau M, Belair J, Brunengraber H. 1987. Production of acetone and conversion of acetone to acetate in the perfused rat liver. J Biol Chem 262:6735–6740.

Hall JD, Mackenzie NE, Mansfield JM, McCloskey DE, Scotts AI. 1988. ^{13}C-NMR analysis of alanine metabolism by isolated perfused livers from C3HeB/FeJ mice infected with African trypanosomes. Comp Biochem Physiol 89B:679–685.

Hill RJ, Hobbs DC, Koeppe RE. 1958. The incorporation of noncarboxyl carbon into glutamic acid, alanine, and aspartic acid by the rat. J Biol Chem 230:169–178.

Jans AWH, Leibfritz D. 1988. A ^{13}C-NMR study on the influxes into the tricarboxylic acid cycle of a renal epithelial cell line, LLC-Pk1/Cl_4: The metabolism of [2-^{13}C]glycine, L-[3-^{13}C]alanine and DL-[3-^{13}C]aspartic acid in renal epithelial cells. Biochim Biophys Acta 970: 241–250.

Jans AWH, Willem R. 1988. ^{13}C-NMR study of glycerol metabolism in rabbit renal cells. Eur J Biochem 174:67–73.

Jans AWH, Willem R. 1989. A ^{13}C-NMR investigation of the metabolism of amino acids in renal proximal convoluted tubules of normal and streptozotocin-treated rats and rabbits. Biochem J 263:231–241.

Kam W, Kumaran K, Landau BR. 1978. Contribution of ω-oxidation to fatty acid oxidation by liver of rat and monkey. J Lipid Res 19: 591–600.

Klapa MI, Park SM, Sinskey AJ, Stephanopoulos GN. 1999. Metabolite and isotopomer balancing in the analysis of metabolic cycles: I. Theory Biotechnol Bioeng 62:375–391.

Kosugi K, Chandramouli V, Kumaran K, Schumann W, Landau BR. 1986. Determinants in the pathways followed by the carbons of acetone in their conversion to glucose. J Biol Chem 261:13179–13181.

Narbad A, Hewlins MJE, Callely AG. 1989. ^{13}C-NMR studies of acetate and methanol metabolism by methylotrophic Pseudomonas strains. J Gen Microbiol 135:1469–1477.

Owen OE, Trapp VE, Skatches CL, Mozzoli MA, Hoeldtke RD, Boden G, Reichard GA. 1982. Acetone metabolism during diabetic ketoacidosis. Diabetes 31:342–348.

Reichard GA, Haff AC, Skutches CL, Paul P, Holroyde CP, Owen OE. 1979. Plasma acetone metabolism in the fasting human. J Clin Invest 63:619–626.

Reichard GA, Skutches CL, Hoeldtke RD, Owen OE. 1986. Acetone metabolism in humans during diabetic ketoacidosis. Diabetes 35: 668–674.

Sakami W, Lafaye JM. 1951. The metabolism of acetone in the intact rat. J Biol Chem 193:199–203.

Schumann WC, Magnusson I, Chandramouli V, Kumaran K, Wahren J, Landau BR. 1991. Metabolism of [2-^{14}C]acetate and its use in assessing hepatic Krebs cycle activity and gluconeogenesis. J Biol Chem 266:6985–6990.

Sulway MJ, Malins JM. 1970. Acetone in diabetic ketoacidosis. Lancet 1:736–740.

Tran-Dinh S, Hervé M, Lebourguais O, Jerome M, Wietzerbin J. 1991. Effects of amphotericin B on the glucose metabolism in Saccharomyces cerevisiae cells. Studies by ^{13}C, ^{1}H-NMR and biochemical methods. Eur J Biochem 197:271–279.

Walker TE, London RE. 1987. Biosynthetic preparation of L-[^{13}C]- and [^{15}N]glutamate by Brevibacterium flavum. Appl Environ Microbiol 53:92–98.

Walsh K, Koshland DE. 1984. Determination of flux through the branch point of two metabolic cycles. The tricarboxylic acid cycle and the glyoxylate shunt. J Biol Chem 259:9646–9654.

Wood HG, Stjernholm R. 1961. Transcarboxylase: II. Purification and properties of methylmalonyloxaloacetic transcarboxylase. Proc Natl Acad Sci USA 47:289–303.